

Reynolds Stress Models for Shock-Turbulence Interaction



Sebastian Karl, Jean-Pierre Hickey, and Francis Lacombe

Abstract A systematic deficiency of current turbulence models which are based on the Reynolds-averaged Navier-Stokes equations (RANS) is their inability to correctly predict the interaction of turbulence with shocks. This is because RANS models do not account for the unsteady motion or fragmentation of the shock wave within the interaction zone. Typically, significant over-prediction of the turbulent energy amplification occurs without dedicated adjustment of the applied turbulence model.

An empirical shock correction for Reynolds stress models (RSM) is proposed. This corrective model is based on rescaling of the production and redistribution terms in the Reynolds stress and length scale equations. The method is tested for two common RSM models and enables them to correctly predict the turbulence amplification, anisotropy, and dissipation downstream of the interaction with a normal shock wave.

1 Introduction

Many problems in super- and hypersonic aerodynamics are characterized by large Reynolds numbers. The application of turbulence models based on the Reynolds-averaged Navier-Stokes equations (RANS) is still required for the computational analysis of such flows because the application of scale-resolving methods results in prohibitive computational cost. Reynolds stress models (RSM) represent a

S. Karl (✉)

DLR – Institute of Aerodynamics and Flow Technology, Göttingen, Germany

e-mail: sebastian.karl@dlr.de

J.-P. Hickey

University of Waterloo, Department of Mechanical and Mechatronics Engineering, Waterloo, QC, Canada

F. Lacombe

Ecole Polytechnique de Montreal, Department of Mechanical Engineering, Montreal, QC, Canada

particularly accurate method for the modeling of turbulence in super- and hypersonic flows. Their ability to resolve anisotropy of the Reynolds stress tensor as well as effects of flow history enables them to capture additional properties of turbulence which are characteristic for many high-speed flows.

However, the RSM approach suffers, as RANS models in general, from severe over-prediction of Reynolds stress amplification due to the interaction of turbulence and shock waves. Further, source terms in the transport equations for the turbulent kinetic energy or Reynolds stresses contain non-conservative derivatives of the flow variables. This induces additional grid convergence problems in the vicinity of a turbulence/shock interaction.

Shock-turbulence corrections which are available to date are limited to two-equation eddy-viscosity models. These approaches are either based on empirical rescaling of production terms [1, 2] or a conservative reformulation of the k-epsilon model [3].

The present work aims at extending the empirical rescaling approach to RSM models. The developed method is applied to the Wilcox stress-omega [4] and the SSG/LRR-omega [5] models. The Menter baseline omega equation [6] is used to predict the turbulent length and time scale in both cases.

Recent DNS data for canonical shock-turbulence interaction [7] is used to derive the mathematical form and to adjust the model constants of the rescaling operators for a wide range of Mach numbers.

2 General Observations from DNS Data

The interaction of turbulence with a shock is characterized by very small length and time scales which impede detailed experimental or numerical investigations. Only the recent availability of DNS data [7, 8] enables a detailed study of this phenomenon. Results from Larsson et al. [7] which cover a range of Mach numbers, M , between 1.05 and 6; of turbulent Mach numbers, M_t , between 0.05 and 0.38; and of Reynolds numbers based on the dissipation length scale, Re_L , between 180 and 670 were used as the basis for the derivation of the present RSM correction model.

The amplification of turbulent kinetic energy (ratio of the values downstream and upstream of the shock, k^d and k^u) from the DNS data is shown in Fig. 1. The scatter of the symbols in the left part of the figure is due to different values of Re_L and M_t for the same shock Mach number. This scatter is significantly reduced if the turbulent energy amplification is plotted against the difference of the upstream and the turbulent Mach numbers, $M - M_t$, as shown in the right part of the figure. Further, the amplification factor can be approximated with the sum of two exponential functions in Eq. (1). The result of Eq. (1) is shown as a $F(M - M_t)$ in Fig. 1.

$$\frac{k^d}{k^u} = k_1 \exp(k_2 (M - M_t)) - k_3 \exp(k_4 (M - M_t)) \quad (1)$$

$$k_1 = 1.533; \quad k_2 = 0.009267; \quad k_3 = 2.355; \quad k_4 = -1.526$$

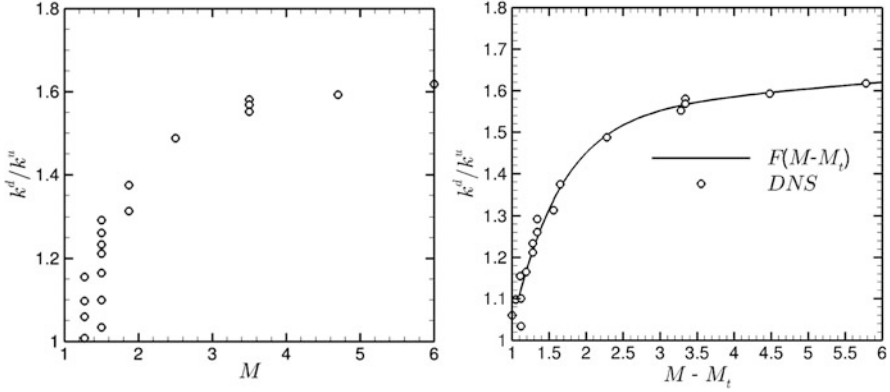


Fig. 1 Amplification of turbulent kinetic energy due to a normal shock from DNS data [7]

3 Shock Correction for Reynolds Stress Models

The RSM shock correction model for CFD is designed based on the two main observations from Sect. 2. The turbulence amplification can be approximated with the sum of two exponential functions, and the argument of these functions should be the difference of shock Mach number and turbulent Mach number. The model constants were determined by systematic comparison of CFD-RANS results with reference data from DNS. The consequent model is summarized in Eqs. (2) and (3). Equation (2) shows the general transport equations for the Reynolds stresses, R_{ij} , and the specific dissipation rate, ω . The differences between the considered RSM models are related to different formulations of the redistribution terms Π_{ij} . The correction of the RSM models is achieved by rescaling of the production and redistribution terms in the Reynolds stress transport equations with the scalar factors K_P and K_Π . Further, the production term of the specific turbulent dissipation rate is scaled by the factor K_ω . All scaling factors are defined in Eq. (3) and depend only on the Mach number, M , and the turbulent Mach number, M_t , upstream of the shock. At Mach numbers below unity, all scaling factors are one, and the correction model is switched off. The validity of this formulation was not tested for extreme Mach numbers, i.e., at Mach numbers above 45, K_P becomes negative, and, for practical implementation, a limitation becomes necessary.

$$\begin{aligned}
 \frac{\partial(\bar{\rho}\tilde{R}_{ij})}{\partial t} + \frac{\partial(\bar{\rho}\tilde{u}_k\tilde{R}_{ij})}{\partial x_k} &= \mathbf{K}_P\bar{\rho}P_{ij} + \mathbf{K}_\Pi\bar{\rho}\Pi_{ij} - \frac{2}{3}\beta^*\bar{\rho}\omega\tilde{\delta}_{ij} + \frac{\partial}{\partial x_k} \left[(\mu + \sigma^*\mu_t) \frac{\partial\tilde{R}_{ij}}{\partial x_k} \right] \\
 \frac{\partial(\bar{\rho}\omega)}{\partial t} + \frac{\partial(\bar{\rho}\tilde{u}_k\omega)}{\partial x_k} &= \mathbf{K}_\omega\gamma\frac{2\omega}{\tilde{R}_{kk}}\tilde{R}_{ij}\frac{\partial\tilde{u}_i}{\partial x_j} - \beta\bar{\rho}\omega^2 + \frac{\partial}{\partial x_j} \left[(\mu + \sigma_\omega\mu_t) \frac{\partial\omega}{\partial x_j} \right] + \text{CD}
 \end{aligned} \tag{2}$$

$$\begin{aligned}
 K_P &= 1 - \max \left[0; k_1 \left(k_2 - \exp \left(k_3 \tilde{M} \right) - \exp \left(k_4 \tilde{M} \right) \right) \right] \\
 K_\Pi &= K_P; \quad K_\omega = K_P^{-1/6}; \quad \tilde{M} = 1 - (M - M_t) \\
 k_1 &= 0.63; \quad k_2 = 2.0; \quad k_3 = 1.2; \quad k_4 = 0.02
 \end{aligned}
 \tag{3}$$

The implementation of the correction model requires a shock sensor. A formulation based on the pressure gradient was used, and compression was identified by comparing the direction of the flow velocity with the pressure gradient. The shock-normal Mach number, M , was computed using the velocity component aligned with the direction of the pressure gradient.

The Mach number upstream of the shock, M , is the main parameter which controls the source term rescaling. Hence, a major drawback of the proposed model is the violation of Galilean invariance. Application to unsteady flows with significant shock motion requires additional considerations. This drawback is also applied to established correction methods for two-equation eddy-viscosity models [1, 2].

4 Validation and Assessment of the Shock Correction Method

The design, validation, and assessment of the RSM shock correction model were based on the CFD analysis of a canonical interaction of isotropic turbulence with a normal shock using the DLR Tau code [9]. To model this interaction with a steady-state CFD approach, a two-dimensional computational model as shown in Fig. 2 was used.

Supersonic flow conditions were imposed by a Dirichlet inflow boundary condition. The static pressure downstream of the normal shock was set at the subsonic pressure outlet. Inviscid slip walls were used at the channel walls. A diverging section with wall angles of 0.3° was added to stabilize the shock position in the CFD solution. The compressible Favre-averaged Navier-Stokes equations for a calorically perfect gas were solved. The ratio of specific heats was 1.4, and the viscosity was approximated using Sutherland's law. Inflow properties are set to match the Mach and Reynolds numbers of the DNS results [7]. The boundary conditions for the turbulence model equations were approximated from the turbulent Mach number, M_t , and the dissipation length scale Reynolds number, Re_L , using Eqs. (4) and (5). First, the turbulent quantities upstream of the shock are computed

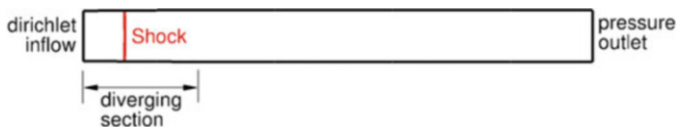


Fig. 2 Schematic of the computational domain

with Eq. (4). Then, the values at the inflow are estimated using Eq. (5). The constants $\beta = 0.09$ and $\beta^* = 0.083$ are taken from the applied turbulence model. The length x corresponds to the distance between the shock and the inflow boundary

$$\omega_x = \frac{\rho(M_t a)^2}{\sqrt{6}\beta^*\mu\text{Re}_L}; \quad k_x = \frac{1}{2}(M_t a)^2 \quad (4)$$

$$\omega_0 = \frac{\omega_x}{1 - \frac{1}{u_0}\omega_x\beta x}; \quad k_0 = \left(1 + \omega_0\beta x \frac{1}{u_0}\right)^{\frac{\beta^*}{\beta}} \quad (5)$$

Comparisons between the RANS results with and without shock correction and the corresponding DNS data are shown in Fig. 3 for the Wilcox model and in Fig. 4 for the SSG/LRR model. The shock-normal and tangential Reynolds stresses, R_{11} and R_{22} , and the turbulent dissipation rate, ε , are normalized with the values upstream of the shock. The length, x , is normalized with the dissipation length scale L_ε . A summary of the turbulent quantities used in the present analysis is given in Eq. (6).

$$M_t = \frac{\sqrt{R_{kk}}}{a}; \quad L_\varepsilon = \frac{\sqrt{\frac{1}{2}R_{kkk}}}{\beta^*\omega}; \quad \text{Re}_L = \frac{\rho\sqrt{\frac{1}{3}R_{kkk}}L_\varepsilon}{\mu} \quad (6)$$

Extracted quantitative turbulent properties downstream of the turbulence/shock interaction are summarized in Table 1. The measure for the amplification is the ratio of turbulent kinetic energies downstream of the shock at $x/L_\varepsilon = 2$ and upstream of the shock. The anisotropy is assessed by the ratio of shock-normal and tangential Reynolds stresses, R_{11}/R_{22} , at the same location. The measure for the decay of turbulence is the ratio of turbulent kinetic energies at $x/L_\varepsilon = 2$ and $x/L_\varepsilon = 15$.

Both applied RSM models significantly over-predict the turbulence amplification across the shock wave without shock correction at large Mach numbers. The error of the SSG/LRR model for a shock Mach number of 6 is about two orders of magnitude. For low shock numbers up to 1.5, both models are able to capture the evolution of the Reynolds stresses and the turbulent dissipation rate without additional correction.

The proposed shock correction method significantly increases the Mach number range for which the RSM models are applicable. The maximum error of the turbulent energy amplification for all considered cases is reduced from two orders of magnitude to 7%. The quality of the predictions for the anisotropy of the Reynolds stress tensor and the decay rate of the turbulent kinetic energy is retained or slightly improved. The maximum error of the anisotropy is 30% for the corrected model (SSG/LRR, $M = 3.5$) and 32% for the uncorrected model (Wilcox-RSM, $M = 3.5$). The maximum errors of the decay for the corrected and uncorrected models are 23% (SSG/LRR, $M = 1.5$) and 27% (Wilcox-RSM, $M = 6$), respectively.

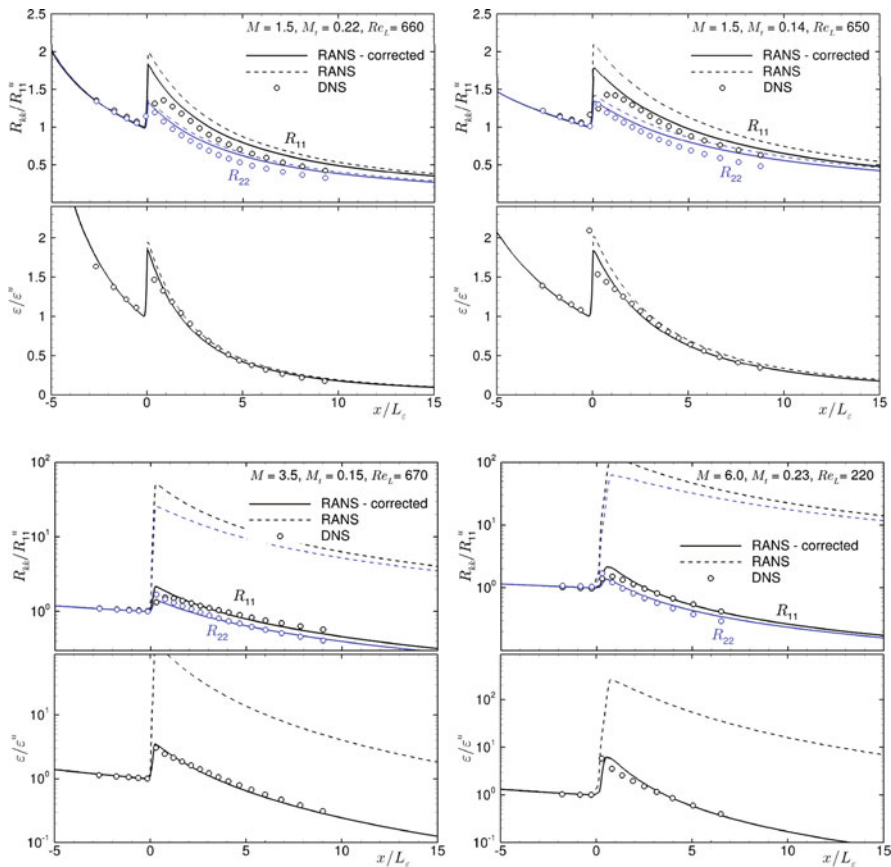


Fig. 3 Distributions of shock-normal and tangential Reynolds stresses and turbulent dissipation rate (Wilcox-RSM model)

5 Conclusion

A shock correction method is proposed to enable accurate prediction of turbulence/shock interaction with Reynolds stress models. The proposed correction is simple to implement, is numerically robust, and enables the considered RSM models to accurately predict the Reynolds stress amplification, decay, and anisotropy downstream of a shock wave. The method was implemented in the DLR Tau code, and obtained CFD results for a canonical turbulence/shock interaction show good agreement with the available DNS reference data.

The major disadvantage of the proposed model is the violation of Galilean invariance. Further work is required to remedy this issue and to analyze the performance of the correction model at inclined shocks.

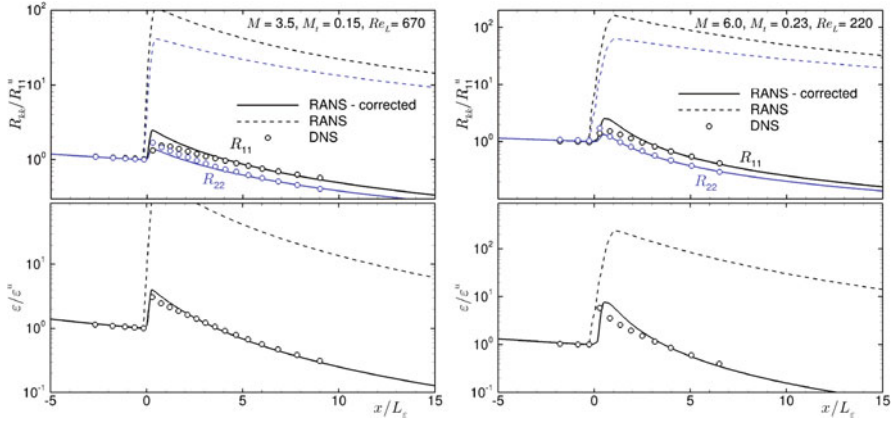


Fig. 4 Distributions of shock-normal and tangential Reynolds stresses and turbulent dissipation rate (SSG/LRR-omega RSM model)

Table 1 Summary of turbulence properties downstream of the shock interaction

Case	Amplification			Anisotropy			Decay		
	$k_d/k_u @ x/L_\epsilon = 2$			$R_{11}/R_{22} @ x/L_\epsilon = 2$			$k_{(x/L_\epsilon = 2)}/k_{(x/L_\epsilon = 15)}$		
S = SSG/LRR	DNS	Corr.	Orig.	DNS	Corr.	Orig.	DNS	Corr.	Orig.
$M = 1.5, M_t = 0.22, W$	0.95	1.01	1.11	1.31	1.28	1.32	0.26	0.31	0.30
$M = 1.5, M_t = 0.14, W$	1.09	1.14	1.30	1.28	1.33	1.39	0.31	0.37	0.38
$M = 3.5, M_t = 0.15, W$	1.17	1.12	20.07	1.19	1.36	1.58	0.26	0.26	0.18
$M = 6.0, M_t = 0.23, W$	0.90	0.97	65.1	1.39	1.42	1.74	0.15	0.17	0.19
$M = 3.5, M_t = 0.15, S$	1.17	1.17	46.9	1.19	1.56	2.25	0.26	0.25	0.23
$M = 3.5, M_t = 0.15, S$	0.90	0.94	85.6	1.39	1.82	2.39	0.15	0.15	0.28

Acknowledgment The authors would like to thank Johan Larsson (University of Maryland) for his advice and help to perform this work.

References

1. K. Sinha, K. Mahesh, G. Candler, *Phys. Fluids* **15**(8), 2290–2297 (2003)
2. K. Sinha, K. Mahesh, G. Candler, *AIAA J.* **43**(3), 586–594 (2005)
3. K. Sinha, S.J. Balasridhar, *AIAA J.* **51**(3), 1872–1882 (2013)
4. D.C. Wilcox, *Turbulence Modeling for CFD* (DCW Industries, La Canada, 2006)
5. R.D. Cecora, R. Radespiel, B. Eisfeld, A. Probst, *AIAA J.* **53**(3), 739–755 (2015)
6. F.R. Menter, *AIAA J.* **32**(8), 1598–1605 (1994)
7. J. Larsson, I. Bermejo-Moreno, S.K. Lele, *J. Fluid Mech.* **717**, 293–321 (2013)
8. J. Ryu, D. Livescu, *J. Fluid Mech. Rapids* **756**, R1 (2014)
9. S. Langer, A. Schwöppe, N. Kroll, *The DLR Flow Solver TAU – Status and Recent Algorithmic Developments*. AIAA Paper 2014-0080 (2014)